Published in final edited form as:
J Immunol. 2011 December 1; 187(11): 6082–6093. doi:10.4049/jimmunol.1004133.

Attenuated atherosclerotic lesions in apoE-Fcγ chain-deficient hyperlipidemic mouse model is associated with inhibition of Th17 cells and promotion of Tregs[1]

Hang Pong Ng[*,‡,3], **Ramona L. Burris**[*], and **Shanmugam Nagarajan**[*,‡,2,3]

[*]Arkansas Children's Nutrition Center, University of Arkansas for Medical Sciences, Little Rock, AR 72202

[‡]Department of Microbiology and Immunology, University of Arkansas for Medical Sciences, Little Rock, AR 72202

Abstract

Though the presence of anti-oxLDL IgG is well documented in clinical and animal studies, the role for FcγRs to the progression of atherosclerosis has not been studied in detail. In the present study, we investigated the role for activating FcγR in the progression of atherosclerosis using apoE-Fcγ chain double knockout (DKO) mice. Relative to apoE KO mice, arterial lesion formation was significantly decreased in apoE-Fcγ chain DKO mice. Bone marrow chimera studies showed reduced lesions in apoE KO mice receiving the bone marrow of apoE-Fcγ chain DKO mice. Compared to apoE KO mice, anti-oxLDL IgG1 (Th2) and IgG2a (Th1), IL-10, and IFN-γ secretion by activated T cells were increased in apoE-Fc γ chain DKO mice. These findings suggest that reduced atherosclerotic lesion in apoE-Fcγ chain DKO mice is not due to Th1/Th2 imbalance. Interestingly, number of Th17 cells and the secretion of IL-17 by activated CD4+ cells were decreased in apoE-Fcγ chain DKO mice. Notably, the number of T-regulatory cells, expression of mRNA, and secretion of TGF-β and IL-10 were increased in apoE-Fcγ chain DKO mice. Furthermore, secretions of IL-6 and STAT-3 phosphorylation essential for Th17 cell genesis were reduced in apoE-Fcγ chain DKO mice. Importantly, decrease in Th17 cells in apoE-Fcγ chain DKO mice was due to reduced IL-6 release by antigen presenting cells of apoE-Fcγ chain DKO mice. Collectively, our data suggest that activating FcγR promotes atherosclerosis by inducing Th17 response in the hyperlipidemic apoE KO mouse model.

INTRODUCTION

One of the risk factors implicated in the pathogenesis of atherogenesis is an elevated level of low-density lipoprotein (LDL)[4] that leads to the generation of oxidized LDL (oxLDL) (1). OxLDL induces an autoimmune response as evidenced by the presence of anti-oxLDL IgG in atherosclerotic lesions in the hyperlipidemic mouse model (2, 3) and in humans (4–6). These studies have suggested that the titer of autoantibodies against oxLDL correlates with

[1]Supported by NIH grant R01HL086674 (SN).

[2]To whom correspondence to be addressed: Department of Microbiology and Immunology, University of Arkansas for Medical Sciences, Arkansas Children's Nutrition Center, Room N2021C, 15 Children's Way, Little Rock, AR 72202. Phone: 501-364-2814; Fax: 501-364-3161; NagarajanShanmugam@uams.edu.
[3]Present Address: Department of Pathology, University of Pittsburgh School of Medicine, Pittsburgh, PA 15261. NagarajanS@upmc.edu

[4]Abbreviations used in this paper: ApoE KO, apolipoprotein E single knockout; BMT, bone marrow transplantation; DKO, double knockout; LDL, low-density lipoprotein; LDLR KO, LDL receptor single knockout, oxLDL, oxidized-LDL; MDALDL, malondialdehyde modified-LDL; MDALDL-IC, MDALDL immune complex oxLDL-IC, oxLDL immune complex.

the progression of atherosclerosis. Epidemiological studies have shown that plasma CRP, another FcγR ligand (7), is a marker of progression of atherosclerosis (8, 9). However recent studies using human CRP over expression in hyperlipidemic mouse model showed there was no difference in atherosclerotic lesions. Very recent studies using mouse CRP deficiency in atherosclerosis susceptible hyperlipidemic mouse models showed no reduction in atherosclerosis in mice (10), suggesting there is no direct link between CRP levels and progression of atherosclerosis.

FcγR plays an important role in inflammatory cell activation, clearance, and presentation of antigen and also in maintaining immunoglobulin homeostasis (11–13). In mice, four different classes of FcγRs have been recognized: FcγRI, FcγRII, FcγRIII, and FcγRIV (11–13). Functionally, FcγRs can be classified into the activating (FcγRI, III and IV) and inhibitory (FcγRII) receptors (11–13). Fcγ chain is the signaling subunit that co-associates with the activating FcγRs, and assembly and cell-surface expression of the activating FcγRs (FcγRI, III and IV) require the co-expression of Fcγ chain (14, 15). IC binding to the extracellular domain of the ligand binding subunit of the activating FcγRs results in phosphorylation of the ITAM motifs resides in the cytoplasmic domain of Fcγ chain subunit (11–13). On the contrary, FcγRII, an inhibitory FcγR, is a single subunit protein, and IC binding to FcγRII induces a negative signal through its ITIM in the cytoplasmic domain (11–13). Earlier studies have presented evidence that mice deficient in Fcγ chain are resistant to the onset of IC-mediated chronic inflammatory diseases (16, 17).

Activated T cells specific for oxLDL are present in human atherosclerotic plaques, suggesting the involvement of adaptive immune response (18) in the initiation and progression of atherosclerosis. Elevated levels of anti-oxLDL IgG, particularly IgG1 and IgG2a, have been observed in apoE knock out (KO) mice fed hyperlipidemic diet (19). The binding of anti-oxLDL IgG to oxLDL can result in the formation of soluble oxLDL immune complexes (oxLDL-IC). Using an in vitro cell culture model, we have shown that monocytes adhere to oxLDL-IC-deposited on vascular endothelial cells in vitro via FcγR and this interaction leads to induction of pro-inflammatory cytokines and chemokines involved in monocyte recruitment (20). Moreover recent human genetic study identified an association between the activating $Fc\gamma RIIa^{R131}$ polymorophism to the occurrence of acute coronary syndrome (21), suggesting FcγR, activating FcγR may be an important contributor to atherosclerosis. These results suggested that FcγR interaction with oxLDL-IC could contribute to the progression of atherosclerosis. Deletion of the Fcγ chain in apoE KO mice (22) and FcγRIII in LDL receptor KO (LDLR KO) background (23) decreased atherosclerosis while deficiency of FcγRIIb, an inhibitory FcγR, in LDLR and apoE KO showed exacerbated lesions (24, 25). The reduced lesions observed in apoE-Fcγ chain DKO mice were attributed to the decreased ratio of activating vs. inhibitory FcγRs in vascular smooth muscle. Adoptive transfer of CD4+ T cell specific to oxLDL has been shown to promote atherosclerotic lesions by increasing Th1 cells responses (26, 27), suggesting that CD4+ T cells, specifically Th1 cells, play an important role in promoting atherosclerosis. Though these studies have provided the importance of activating FcγR in the progression of atherosclerosis, the relationship between FcγR expressed on inflammatory cells including APC and its effect on CD4+ cells, particularly Th1/Th2 responses, in the development of atherosclerosis remains unexplored.

In this report, we tested the hypothesis that oxLDL-IC binding to activating FcγRs may promote the initiation and progression of atherosclerosis using apoE-Fcγ chain DKO mice by altering CD4+ T cell responses. We show that apoE-Fcγ chain DKO mice developed fewer atherosclerotic lesions. Moreover, bone marrow chimera approach showed attenuated lesions in apoE KO receiving bone marrow from apoE-Fcγ chain DKO mice. We demonstrated that apoE-Fcγ chain DKO mice revealed significant decrease in secretion of

Th17-related cytokine (IL-17 and IL-6). In contrast, the number of T-regulatory cells (Tregs) and expression of TGF-β and Foxp3, Treg-related cytokine and transcription factor, respectively, was increased in apoE-Fcγ chain DKO mice as compared with apoE KO mice. These findings suggest a potential role for the activating FcγRs in generation and differentiation of Th17 response, which has been suggested to contribute to the pathogenesis of atherosclerosis.

MATERIALS AND METHODS

Mice

ApoE KO mice on a C57BL/6 background were purchased from Jackson Laboratory (Bar Harbor, ME). ApoE KO and Fcγ chain KO (Jackson Labs), both in C57BL/6 background, were mated, and F1 progeny (apoE+/−Fcγ chain+/−, heterozygous) were mated to generate apoE-Fcγ chain DKO mice. ApoE KO and apoE-Fcγ chain DKO mice (5 weeks of age) were fed high-fat Western diet (TD 05576, Harlan Laboratories, Madison, WI) or normal chow diet (TD06715, Harlan) for 10 or 20 weeks, respectively. This study was reviewed and approved by the Institutional Animal Care and Use Committee at University of Arkansas for Medical Sciences.

Tissue preparation and morphometric determination of atherosclerosis

Mice were anesthetized with isoflurane before euthanization. Animals were sacrificed at 15 wk (high-fat diet) or 25 wk (chow diet) of age, and blood was collected by the cardiac puncture into heparin-coated tubes. Plasma was separated and stored at −80°C until further analysis. The heart and descending aorta were excised and fixed in aPBS/4% formalin/30% sucrose overnight before mounted in OCT medium and frozen at −70°C. Aortic sinus cryosections (10 μm) were stained with Oil Red O (28). For quantitative analysis of atherosclerosis, the percent lesion area in each of five sections from each mouse was obtained. En face preparations of the descending aorta were washed in distilled water; en face analysis of the descending aorta was performed after staining descending aorta with Sudan IV as previously described (28).

Bone marrow chimera

The recipient apoE KO mice (male, 8 wk) received bone marrow from either apoE KO or apoE-Fcγ chain DKO mice. After bone marrow transplantation (BMT), mice were fed chow diet for 4 weeks. Four weeks after BMT, mice were fed a high-fat diet (TD05576) for another 10 weeks. Genomic DNA was obtained from circulating white blood cells in all mice 4 weeks after BMT. PCR was performed to confirm absence of Fcγ chain using primers specific for Fcγ chain wild type and mutant. The following primers were used: oIMR0618: ctcgtgctttacggtatcgcc (mutant), oIMR0621: accctactctactgtcgactcaag (common), and oIMR0622: ctcacggctggctatagctgcctt (wild type). The PCR amplified products 224 bp (wild type) and 260 bp (mutant) was visualized on 2% agarose gels.

Immunohistochemistry

Serial aortic sinus cryosections (10 μm) were stained with anti-mouse monocyte/macrophage monoclonal antibody (MOMA-2, 1:25 dilution, AbD Serotec, Raleigh, NC) followed by Vectastain ABC reagent (Vector Labs, Burlingame, CA). The sections were developed with DAB and counterstained with Mayer’s hematoxylin. Images were captured using a Carl Zeiss inverted microscope.

Plasma lipid analyses

Concentrations of plasma total and HDL cholesterol were determined by enzymatic methods using kits from BioVision (Mountain view, CA) as described earlier (28).

Stimulation of CD4+ T cells

CD4+ T lymphocytes were purified from splenocytes by positive selection using anti-CD4 microbeads (Miltenyi, Auburn, CA), as recommended by the manufacturer. The purity of CD4+ cells was >99% as determined by FACS analysis using anti-CD4-APC. Purified CD4+ cells (1×10^6) were stimulated with 5 μg/ml plate-bound anti-CD3 mAb (Hamster IgG1, clone 145-2C11, BD Biosciences, San Diego, CA) in presence of 1 μg/ml soluble anti-CD28 mAb (Hamster IgG2, clone 37.51, BD Biosciences) for 48 h. Supernatants were collected to determine cytokines secreted by activated T cells.

Preparation of plate-bound immune complex (pb-IC)

Plate bound OVA-IC and MDALDL-IC were prepared incubating OVA or MDALDL with saturating concentration of affinity purified rabbit anti-OVA IgG and rabbit anti-MDA IgG, respectively. Plate bound IC were prepared by coating OVA or MDALDL at 15 μg/ml in PBS for 1 h at 37°C, followed by blocking with 10% FCS (Hyclone) in PBS for 1 h and a further 1 h incubation with saturating concentration of rabbit anti-OVA or rabbit anti-MDA IgG (10 μg/ml) in PBS/10% FCS. Parallel wells prepared with OVA/anti-MDA IgG and MDALDL/anti-OVA IgG was used as controls. Formation of pb-OVA-IC or pb-MDALDL-IC was confirmed by ELISA using HRP conjugated anti-rabbit IgG.

BMDM and BMDC preparation and IC activation

BMDC were prepared from bone marrow cells (2×10^6 cells/100 mm dish) after incubation with RPMI 1640/10% FBS/mGM-CSF (20 ng/ml, Peprotech) for 6 days (29). Fresh medium with GM-CSF was replaced after 3 days. After 6 days, non-adherent BMDC was collected and used for IC-mediated activation. BMDM were prepared by incubating bone marrow cells in RPMI/10% FBS supplemented with 30% L929 culture supernatant (source of M-CSF) for 6 days (30). BMDM were gently detached using ice-cold PBS. For IC activation, BMDC or BMDM was added to pb-IC and incubated for 24 h. Supernatant was collected to determine IC-mediated secretion of TNF-α, IL-6, IL-12, and IFN-γ. Cells added to wells with antigen alone or antigen with control rabbit IgG were used as controls.

Cytokine analysis—Cytokine secretion in supernatants from anti-CD3/CD28-stimulated CD4+ cells were analyzed using mouse Th1/Th2/Th17 (IL-2, IL-4, IL-6, IFN-γ, TNF-α, IL-17A, and IL-10) cytokine bead array according to the manufacturer's instructions (BD Biosciences). Beads were analyzed using FACSCalibur flow cytometer and FCAP array CBA software (BD Biosciences). Murine TGF-β levels in the supernatant from anti-CD3/CD28 stimulated CD4+ cells, IL-12 and IFN-γ secretion by activated BMDM and BMDC were determined by corresponding Duoset ELISA kit (R&D System Inc., Minneapolis, MN).

Quantitative RT-PCR analysis

The aorta was perfused with nuclease-free PBS. Total RNA was isolated from a proximal portion of the descending aorta (aortic arch and aorta proximal to the subclavian artery) and spleen using TRIzol (Invitrogen, Carlsbad, CA) according to the manufacturer's instructions. RNA was quantified using Nanodrop spectrophotometer (Nanodrop Products, Wilmington, DE), and its integrity was determined using BioRad Experion RNA analyzer (BioRad, Hercules, CA). Gene expression was measured by real-time RT-PCR after reverse transcription of total RNA (0.5 μg) as described earlier (28). PCR primer pairs were

purchased from SA-Biosciences (Frederick, MD). Two-step PCR with denaturation at 95°C for 15 s and annealing and extension at 60°C for 1 min for 40 cycles was conducted in iCycler (BioRad). Expression of target gene was calculated by $^{\Delta\Delta}$Ct method using threshold cycles for β-actin as normalization reference. All real-time PCR reactions were carried out at least twice from independent cDNA preparations. RNA without reverse transcriptase served as a negative control.

Determination of MDALDL Antibody

Malondialdehyde-LDL (Academy Biomedical Company Inc., Houston, TX) and anti-MDALDL IgG and IgM responses were determined by method described earlier (26). Briefly, MDALDL (10 μg/ml in PBS/1 mM EDTA) was coated on Microfluor white plates overnight at 4°C and blocked with PBS/1% BSA/1 mM EDTA for 2 h at room temperature. Sera (1–50 diluted) was added to the plate and incubated at room temperature for 2 h. Plates were washed, and then alkaline phosphatase (AP)-conjugated anti-mouse IgG1, anti-mouse IgG2a, anti-mouse IgG2b, anti-mouse IgG3, or anti-mouse IgM (Southern Biotech, Birmingham, AL) was added and incubated for 1 h at room temperature. The AP enzymatic activity was determined using luminescence substrate, Lumi-Phos530 (Lumigen Inc. Southfield, MI), and luminescence was read at 530 nm in a Polarstar plate reader (BMG Labtech Inc., Cary, NC).

Flow cytometric analysis of T cell subsets

Splenocytes (3×10^5 cells) were stained with T-lymphocyte subset antibody cocktail (BD Biosciences), and different T cell subsets were analyzed in a FACSCalibur flow cytometer followed by data analysis using FlowJo analytical software (Tree Star Inc., Ashland, OR). T lymphocyte subset antibody cocktail consists of the PE-Cy7-anti-CD3e (clone 145-2C11), PE-anti-CD4 (clone RM4–5), and APC-anti-CD8a (clone 53-6.7). Cells stained with corresponding isotype IgG were used as controls. To determine CD152+/CD4+ T cells, splenocytes were stained with APC-anti-CD4, PE-Cy5-CD25, and PE-CTLA4 and were analyzed by flow cytometry. For Treg cells analysis, splenocytes were incubated with APC-anti-CD4 and PE-Cy5-anti-CD25. After surface staining, cells were fixed and permeabilized and stained with PE-anti-Foxp3 according to the manufacturer's instructions (BD Bioscience). For Th17 cell analysis, purified CD4+ cells (10^6 cells/ml) were incubated with 50 ng/ml PMA and 1 μM ionomycin for 6 h in the presence of monensin. Then cells were stained with APC-anti-CD4 at 4°C for 20 min. Cells were fixed and permeabilized and stained with PE-anti-IL-17A mAb. Cells stained with isotype control IgG were used as controls. Cells were analyzed by flow cytometric analysis using a FACSCalibur flow cytometry equipped with CellQuest software (BD Biosciences, San Jose, CA). Percent positive cells were determined using FlowJo software.

Assay for p-Stat3

CD4+ T cells were stimulated with anti-CD3/CD28 mAb as described earlier and lysed in lysis buffer containing protease and phosphatase inhibitors (Cell Signaling Technologies Inc., Danvers, MA). To determine IL-6 dependent STAT3 phosphorylation CD4+ T cells were stimulated with IL-6 (20 ng/ml) for 30 min. Levels of pSTAT3 and total STAT3 in the cell lysates were determined using Pathscan ELISA kits specific for each one (Cell Signaling). Color was developed using TMB-1 substrate, and the reaction was stopped with 2N sulfuric acid. Absorbance was read at 450 nm in a Polarstar multiplate reader (BMG Labtech). Phospho-STAT3 levels were normalized to total STAT3 levels in each sample.

Statistical analyses

Values are expressed as mean ± SD. Differences between the groups were considered significant at $p<0.05$ using the 2-tailed Student's t test. All data were analyzed using GraphPad InStat version 3.1a for Macintosh (GraphPad Software, San Diego, CA).

RESULTS

ApoE-Fcγ chain DKO mice show reduced atherosclerotic lesions

To determine the role of activating FcγRs in the progression of atherosclerosis, total activating FcγR deficiency in apoE KO background was generated. Genotype analyses showed complete knockout for Fcγ chain in apoE KO background (Fig. 1A). Spontaneous atherosclerotic lesions in apoE KO and apoE-Fcγ chain DKO mice fed chow diet (contains 5% fat with no cholesterol) were determined by staining aortic sinus cryosections (10 μm) with Oil Red O (Fig. 1B). Atherosclerotic lesions in aortic tree were performed by staining descending aorta from the aortic arch to the iliac bifurcation with Sudan IV (Fig. 1C). Both analyses showed approximately a 50% reduction in lesions ($P<0.01$, Student's *t* test) in apoE-Fcγ chain DKO mice compared to apoE KO mice (Fig. 1D). We then determined whether Fcγ chain deficiency also had an effect on accelerated atherosclerosis in mice fed high-fat diet (21% fat and 0.15% cholesterol). ApoE KO mice showed more lesions in the aortic sinus (Fig 1E and F) while Fcγ chain deficiency was associated with a significant decrease in lesion area in the aortic root and aortic arch relative to apoE KO male mice (Fig. 1E and F). Female apoE-Fcγ chain DKO mice also showed similar reduction in lesions suggesting there is no effect of gender on the extent of lesions (data not shown). Since Fcγ chain is essential for expression and assembly of FcγRI, FcγRIII, and FcγRIV (activating FcγRs), these findings suggest activating FcγRs contribute to the atherosclerotic lesion formation.

Activating FcγR expressed on hematopoietic cells is sufficient to contribute to the atherosclerotic lesions

Studies using human cell lines have shown the expression of FcγR in vascular endothelial and smooth muscle cells (31, 32). Next we investigated whether activating FcγRs expressed on cells of hematopoietic origin contribute to the progression of atherosclerosis by bone marrow chimera. Bone marrow cells from apoE KO or apoE-Fcγ chain DKO mice were transplanted to apoE KO recipient mice. Deletion of the Fcγ chain in hematopoietic cells was confirmed by the genomic PCR analyses (Fig. 2A). ApoE KO mice transplanted with apoE KO bone marrow cells showed significantly increased atherosclerotic lesions in the aortic root (Fig. 2B and D). However, apoE KO mice transplanted with apoE-Fcγ chain DKO bone marrow cells revealed a reduction of more than 50% ($p<0.01$) in atherosclerotic lesions (Fig. 2B and D). Immunohistochemical analyses showed reduced macrophage at the lesions in apoE-Fcγ chain DKO chimera than in apoE KO chimera mice, suggesting reduced monocyte migration and subsequent transformation to macrophages at the lesion site. Moreover, analyses of mRNA expression of macrophage FcγRIIB (inhibitory) and the activating FcγR (FcγRI, III, and IV) did not reveal any difference in the ratio between the activating and inhibitory FcγRs expression in inflammatory cells (data not shown). These findings suggest that activating FcγR expression on hematopoietic cells is sufficient to contribute the atherosclerotic lesions.

Fcγ chain deficiency does not alter plasma cholesterol levels

To determine the molecular mechanisms contributing to the decreased number of atherosclerotic lesions in apoE-Fcγ chain DKO mice, plasma total and HDL cholesterol levels were determined. There were no differences in plasma lipid profiles in apoE-Fcγ chain DKO mice compared with apoE KO controls fed chow or high fat diet (Table I).

Similar findings were observed in bone marrow chimera mice (Table I). These data suggest that the reduction in lesion formation in apoE-Fcγ DKO mice compared with apoE KO mice was not due to changes in plasma lipid levels.

Anti-oxLDL IgG levels were elevated in apoE-Fcγ chain DKO mice

Anti-oxLDL antibody (IgG and IgM) responses were determined for each isotype at 10 weeks of high-fat diet. The apoE KO mice lacking Fcγ chain expression had significantly higher levels of oxLDL-specific IgG response (Fig. 3A), whereas no difference was found in anti-oxLDL IgM response (Fig. 3B). Anti-oxLDL IgG isotype analyses showed anti-oxLDL IgG2a Abs was elevated several fold, as well as the anti-oxLDL IgG1, IgG2b and IgG3 (Fig. 3C). Ratio of IgG2a/IgG1 was not different between apoE KO and apoE-Fcγ chain DKO mice (Fig. 3D). Similar results were obtained when oxLDL was used in this assay (data not shown). Total plasma IgG and IgM were not different between apoE KO mice and apoE-Fcγ chain DKO mice (data not shown). These findings suggest there was no Th1/Th2 bias in apoE-Fcγ chain DKO mice. These findings suggest there is no apparent increase in Th1/Th2 shift in apoE-Fcγ chain DKO mice.

Attenuated atherosclerotic lesion in apoE-Fcγ chain DKO mice is not due to Th1/Th2 shift

Earlier studies have suggested that CD4+ T cells specific to oxLDL promote lesions by increasing Th1 cell responses (26, 27). To investigate if the Th1/Th2 shift could have contributed to the attenuated lesions in the activating FcγR-deficient mice, cytokine response by activated CD4+ T cells (from high-fat-fed mice) and anti-oxLDL IgG2a (Th1) and IgG1 (Th2) levels were determined. Analysis of CD4+ and CD8+ T cell populations showed there was no difference in CD4+/CD8+ ratio in apoE-Fcγ chain DKO mice and apoE KO mice cells (data not shown). Activated-CD4+ T-cells secreted high levels of IL-10 with no difference in IL-4 levels in apoE-Fcγ chain DKO mice compared to apoE KO mice (Fig. 4A and B). Surprisingly, a 2-fold increase in the secretion of IFN-γ was observed from activated CD4+ T cells of apoE-Fcγ chain DKO mice relative to apoE KO controls (Fig. 4C). Quantitative RT-PCR analyses of CD4+ cells showed mRNA expression of IL-10 and IL-4 was about 3- and 1.5-fold high in apoE-Fcγ chain DKO mice (Fig. 4D). Notably, IFN-γ mRNA levels were also about 3-fold higher in apoE-Fcγ chain DKO compared to apoE KO mice (Fig. 4D). Zhou et al. (19) have shown that IFN-γ mRNA expression was high in the arterial lesion site suggesting that local Th1 response at the lesion site may be contributing to the progression of atherosclerosis. We then investigated whether the change in Th1/Th2 immune responses at the lesion sites may have contributed to the reduction in lesion formation in the apoE-Fcγ chain DKO mice. Using aorta from high-fat-fed mice, we determined the mRNA levels of cytokines in apoE KO and apoE-Fcγ chain DKO mice. Consistent with the changes in cytokine production by activated CD4+ T lymphocytes, mRNA levels for IL-10 in apoE-Fcγ chain DKO were significantly higher relative to apoE KO mice (Fig. 4E). In contrast to the earlier observation (19), IFN-γ mRNA expression in the aorta (at the lesion site) was also higher in apoE-Fcγ chain DKO mice vs. apoE KO mice (Fig. 4E). These findings suggest that Th1/Th2 imbalance may not be contributing to the attenuated atherosclerotic lesions in apoE-Fcγ chain DKO mice. To address whether CD4+ T cells from apoE-Fcγ chain DKO show a bias in Th1/Th2 differentiation intrinsically, basal expression of transcription factors T-bet (Th1) and GATA3 (Th2), which initiate Th1 and Th2 cell development, respectively (33, 34), was analyzed. The mRNA expression of T-bet and GATA-3 in CD4+ T cells of apoE-Fcγ DKO and apoE KO mice were not different (Fig. 4F).

Th17 cells were reduced in apoE-Fcγ DKO mice

We then investigated alternative mechanism(s) that may be contributing to the reduced lesions in apoE-Fcγ chain DKO mice. CD4+ T cells of apoE-Fcγ chain DKO mice showed

about 50% low IL-17 mRNA expression compared to apoE KO mice (Fig. 5A). Moreover, compared to CD4+ cells of apoE KO, IL-17 secretion by CD4+ T cells of apoE-Fcγ chain DKO mice was significantly reduced after stimulation with anti-CD3 and anti-CD28 (Fig. 5B). Then we determined whether Fcγ chain deficiency in hyperlipidemic apoE KO mice resulted in reduced number of Th17 cells. Intracellular staining for IL-17 in PMA/ionomycin-activated CD4+ cells revealed apoE KO mice have about 2% Th17+ cells (Fig. 5C and D). However, the number of Th17+ cells was reduced to less than 0.5% of CD4+ cells in apoE-Fcγ chain DKO mice (Fig. 5C and D). Then we determined the expression of IL-17 in the aorta samples to address whether IL-17 expression is reduced at the lesion site. IL-17A mRNA expression was lower in aorta sample from apoE-Fcγ chain DKO mice (Fig. 5E). These findings suggest that decreased generation of Th17 cells and IL-17 expression in apoE-Fcγ chain DKO mice could in part contribute to the attenuated atherosclerotic lesions in these mice.

More Tregs in apoE-Fcγ chain DKO deficient mice

Recent studies using apoE KO mice have shown that there is an inverse relationship to the number of Th17 and $CD4^+CD25^+Foxp3^+$ regulatory T (Treg) cells (35–37). Hence, we determined the number of Treg cells in apoE KO and apoE-Fcγ chain DKO mice fed a high-fat diet. The deficiency of Fcγ chain in hyperlipidemic apoE KO mice was associated with an increase in the number of Tregs (Fig. 6A). Moreover, about a 2-fold increase in Foxp3 mRNA expression was observed in apoE-Fcγ DKO mice compared with apoE KO mice (Fig. 6B). As CD152 have been shown to be upregulated in Tregs, we determined the mRNA expression of CD152 in the CD4+ T-lymphocytes of apoE KO and apoE-Fcγ chain DKO mice by real-time RT-PCR. Interestingly, CD152 mRNA expression was increased significantly in spleen of apoE-Fcγ chain DKO mice compared with apoE KO mice while expression of CD28, another T cell co-stimulatory molecule, was similar in apoE KO and apoE-Fcγ chain DKO mice (Fig. 6C). These findings suggest that Fcγ chain deficiency in hyperlipidemic mouse background increased the regulatory CD4+ T cell population causing an imbalance between Th17 and Tregs.

Mechanism contributing to the Th17/Tregs shift in apoE-Fcγ chain DKO mice

We then determined mechanisms contributing to the reduced Th17 cells in apoE-Fcγ chain DKO mice. Generation of Th17 cells in mice requires the presence of TGF-β and IL-6 (38–40). Hence, the levels of TGF-β and IL-6 in anti-CD3/CD28 activated CD4+ cells. Activated CD4+ cells of the apoE-Fcγ chain secrete 3-fold higher levels of TGF-β than in activated CD4+ cells of apoE KO mice (Fig. 7A). The decrease in TGF-β secretion also paralleled a more than 3-fold increase in TGF-β mRNA expression in apoE-Fcγ chain DKO mice (Fig. 7B). TGF-β can prime the naïve CD4+ T cells to differentiate into Tregs or Th17 cells depending on the presence of IL-6 (39). Hence, IL-6 secretion by activated CD4+ cells was determined. IL-6 mRNA (Fig. 7C) and IL-6 secretion by activated CD4+ cells (Fig. 7D) was significantly reduced in apoE-Fcγ chain DKO mice. Recent studies showed that the IL-6/STAT3 signaling pathway plays a predominant role in the induction of Th17 response in autoimmune disease (41, 42). Since IL-6 and IL-17 secretion was reduced in anti-CD3 stimulated CD4+ cells from apoE-Fcγ chain DKO mice, we investigated whether STAT3 activation are reduced in apoE-Fcγ chain DKO mice. Total and phospho-STAT3 levels in activated CD4+ T cells were determined by ELISA-based assay. Total STAT3 levels were not different between the two strains of mice (Fig. 7E). However, less p-STAT3 was detected in CD4+ T cells from apoE-Fcγ chain DKO mice when compared to that from apoE KO mice (Fig. 7F). IL-21 selectively produced by Th17 cells has been shown to serve as an autocrine factor for promoting and sustaining Th17 lineage commitment and drive IL-17 production in STAT3-dependent manner (43). Hence, we determined whether lower pSTAT3 in apoE-Fcγ chain DKO mice affect IL-21 secreted by activated T cells. IL-21

secretion in activated T cell was significant lower in apoE-Fcγ chain DKO mice (Fig. 7G) compared to T cells from apoE KO mice. Since we observed both reduced IL-6 and STAT3 phosphorylation in apoE-Fcγ chain mice, we then determined whether Fcγ chain deficiency affect IL-6 signaling pathway, which may lead to IL-17 response. CD4+ T cells were treated with IL-6 and pSTAT3 was detected. Total STAT3 levels were also not different between both strains (data not shown). Basal and IL-6-mediated pSTAT3 levels were not different between apoE KO and apoE-Fcγ chain DKO mice (Fig. 7H), suggesting that Fcγ chain deficiency does not affect IL-6 signaling pathway. These findings indicate that less Th17 response in apoE-Fcγ chain DKO mice may result from lack of optimal cytokine responses such as IL-6 resulting in less activation of STAT3 signaling pathway.

Reduced IL6 secretion by BMDM and BMDC of apoE-Fcγ chain DKO mice

IL-6 release by APC such as DC has been shown to be critical for the generation and differentiation of Th17 cells (44, 45). Hence to identify the FcγR-dependent factors for Th17 skewing in vivo, OVA-IC and MDALDL-IC mediated IL-6 release by BMDM and BMDC of apoE-Fcγ chain DKO mice was determined. Plate-bound OVA-IC or MDALDL-IC was confirmed by ELISA assay prior to adding the cells on IC-coated plates (data not shown). OVA- or MDALDL-treated apoE KO BMDM and BMDC did not induce IL-6 (Fig. 8 A and B) secretion. However, OVA-IC or MDALDL-IC activation of apoE KO BMDM and BMDC showed very high level of IL-6 secretion, about 30-fold for BMDM and 8-fold for BMDC, (Fig. 8A and B). Interestingly, both MDALDL-IC and OVA-IC activation of apoE-Fcγ chain-deficient BMDM and BMDC did not induce IL-6 secretion (Fig. 8A and B). Similar findings were observed for IC-mediated TNF-α (Fig. 8C and D) and IL-12 (Fig. 8E and F) secretion by BMDM and BMDC from apoE-Fcγ chain DKO mice. Under similar conditions INF-γ secretion was too low to be detected (data not shown). These findings suggest that more attenuated Th17 cell in apoE-Fcγ DKO mice may be due to reduced levels of IL-6 secretion by APC deficient in Fcγ chain.

DISCUSSION

In the present study, we tested the hypothesis that oxLDL-IC binding to the activating FcγR promotes the progression of atherosclerosis. We showed a significant reduction in the formation of arterial lesions in Fcγ chain-deficient mice after high-fat diet. Interestingly, bone marrow chimera studies showed attenuated lesions in apoE KO mice transplanted with bone marrow from apoE-Fcγ chain DKO mice. These findings suggest that the activating FcγR expressed on hematopoietic cells is sufficient for the progression of atherosclerosis. Remarkably, the reduction in atherosclerotic lesion progression in the activating FcγR deficiency in hyperlipidemic mouse model was associated with the increased generation of CD4+Tregs with concomitant decrease in CD4+Th17 cells.

Earlier studies have shown expression of activating FcγR in vascular endothelial and smooth muscle cells (31, 32). Moreover, studies using apoE-Fcγ chain DKO mice revealed that expression of the inhibitory FcγRIIB was elevated in vascular smooth muscle cells (19). These studies have suggested that the ratio between inhibitory/activating FcγRs in vascular smooth muscle cells could be responsible for the observed reduced atherosclerotic lesions in apoE-Fcγ chain DKO mice (22). It is well established that both activating and inhibitory FcγRs are constitutively expressed on cells of hematopoietic origin, which include monocytes/macrophages, neutrophils, and NK cells (11–13). Notably, using bone marrow chimera approach, we showed that the deficiency of activating FcγR expression on hematopoietic cells is sufficient to inhibit the progression of atherosclerotic lesions. Thus, the findings from the current study indicate the possibility that the activating FcγR expressed on hematopoietic cells is the major contributor in the progression of atherosclerosis in apoE KO mice.

Th1 response has long been recognized having a proatherogenic potential and an important role in the development of atherosclerosis (19, 26). Plasma anti-oxLDL IgG analyses revealed there is no clear distinction of Th1 (IgG2a) and Th2 (IgG1) type of antibody response in apoE-Fcγ chain DKO mice. Notably, we showed anti-oxLDL IgG1 and IgG2a levels were higher in apoE-Fcγ chain DKO mice compared to apoE KO mice in spite of lesions being lower in apoE-Fcγ chain DKO mice. Earlier studies have shown that in moderate hypercholesterolemia, anti-oxLDL antibody response is predominantly the IgG2a isotype, correlating with increased IFN-γ-producing T cells (19). However severe hypercholesterolemia was shown to be associated with a shift from Th1 to Th2 response as evident from elevated anti-oxLDL IgG1 isotype and appearance of IL-4, Th2 cytokine, producing cells in atherosclerotic lesions (19). These findings suggest that antigenic load may determine the Th1/Th2 autoimmune responses in atherosclerosis. Immunization of apoE KO with MDALDL resulting in elevated plasma anti-oxLDL IgG was atheroprotective (46–48). This raises an interesting possibility that higher anti-oxLDL levels in apoE-Fcγ chain DKO mice may be atheroprotective. However, this possibility needs to be resolved by passive transfer of anti-oxLDL IgG.

Th1 response has long been recognized having a pro-atherogenic potential and an important role in the development of atherosclerosis (19, 26). Our findings showed no difference in IL-4 levels in apoE-Fcγ chain DKO compared with apoE KO mice ruling out a role for IL-4 in reduced lesions in apoE-Fcγ chain DKO mice. Surprisingly, IFN-γ levels were elevated in activated CD4+ T cells of apoE-Fcγ chain DKO mice though the lesions were fewer in these mice. This finding is in agreement with earlier report showing elevated IFN-γ production with attenuated lesion in LDLR-FcγRIII DKO mice (23). The mechanism(s) contributing to the elevated IFN-γ in the total activating FcγR deficiency (our report) and FcγRIII deficiency (23) needs to be explored. To address whether Fcγ chain deficiency inherently influences different T cell subsets, we determined basal level expression of T-bet and GATA-3, transcription factors essential for Th1 and Th2 cell differentiation. We did not detect the difference in T-bet and GATA-3 expression in CD4+ T cells from apoE-Fcγ chain-DKO mice ruling out there is intrinsic effect Fcγ chain deficiency on Th1 and Th2 differentiation. Nevertheless, these findings suggest that the imbalance in Th1/Th2 may not be contributing to the attenuated lesions seen in apoE-Fcγ chain DKO mice. Notably, our findings also showed activated CD4+ T cells produced elevated IL-10 in apoE-Fcγ chain DKO compared with apoE KO mice, suggesting that IL-10 secreted by other T cell subset such as Tregs may be contributing to the reduced lesions in apoE-Fcγ chain DKO mice.

Th17 cells, a subset of CD4 cells secreting IL-17, have been implicated in pro-inflammatory responses (41) suggesting a role for IL-17 in the progression of atherosclerosis. However, the role of IL-17 and Th17 in atherosclerosis is still evolving. The pro-atherogenic role of IL-17 was demonstrated in apoE KO mice using anti-17 mAb (35), recombinant soluble IL-17 receptor-A (36), or LDLR KO recipient mice transplanted with IL-17 receptor deficient bone marrow cells (49) or IL17 KO mice (50). On the contrary, two studies from Mallat group (51, 52) have suggested that the elevated level of IL-17 is athero-protective. In the first study, LDLR KO mice received SOCS3-deficient bone marrow cells showing reduced atherosclerosis with elevated IL-17 and IL-10 level (51). In the second study, the athero-protective role of IL-17 was suggested in B cell-depleted mice showing elevated IL-17 levels (52). It should be pointed out that in all the studies examining the direct role for IL-17 using apoE KO hyperlipidemic mouse model showed IL-17 is pro-atherogenic. Our findings showing reduced lesions, number of Th17 cells, and secretion of IL-17 by activated CD4+ lymphocytes in apoE-Fcγ chain DKO compared to apoE KO mice suggest a pro-atherogenic role for IL17. Moreover, IL-21 selectively produced by Th17 cells has been shown to serve as an autocrine factor for promoting and sustaining Th17 lineage commitment and to drive IL-17 production (43). Our findings showing reduced IL-21

secretion by activated T cells further confirmed that Th17 response is lower in apoE-Fcγ DKO mice. However more studies may be needed to resolve the cloud around the role for IL-17 in atherosclerosis.

Finally, we determined the FcγR-dependent factors that might be a possible mechanism for the reduced Th17 cells in apoE-Fcγ chain-DKO mice. IL-6 and IL-6-dependent STAT3 signaling pathways are essential for Th17 generation (42, 44). We showed IL-6 secretion and STAT3 phosphorylation in activated CD4+ cells was reduced in apoE-Fcγ chain-DKO mice suggesting less IL-6 secretion and STAT3 phosphorylation may relate to reduction of Th17 response in apoE-Fcγ chain-DKO mice. This raises an interesting link between Fcγ chain and IL-6 signaling pathway. However exogenous addition of IL-6 did not show difference in pSTAT3 levels in CD4 cells of apoE KO and apoE-Fcγ chain DKO mice (Fig. 7H) ruled out direct link between Fcγ chain and IL-6 signaling pathway. Previous studies showing DC-derived IL-6 is critical for differentiation (45) raise the possibility that lack of IL6 secretion by APCs from Fcγ chain-deficient mice may affect Th17 differentiation. We showed IC-mediated IL-6 and TNF-α secretion was impaired in BMDM and BMDC from apoE-Fcγ chain-DKO mice, but not from apoE KO mice. Hence, it is possible that in the absence of IL-6, Treg differentiation pathway may be activated rather than Th17 differentiation (53, 54). Recent studies have also shown inverse relationship between Th17 and Tregs cells in the progression of atherosclerosis in hyperlipidemic mouse models (37) and human studies (55–57). We showed deficiency of Fcγ chain resulted in expansion of Treg cells producing high levels of IL-10 and TGF-β, which have been implicated for anti-atherogenic effects (58–60). Collectively, our findings suggest that anti-inflammatory response by CD4+ CD25+ Treg cells may inhibit Th17 differentiation and inhibit the atherosclerosis in hyperlipidemic mouse models.

In summary, our investigation demonstrated that Fcγ chain deficiency leading to the impaired functions of the activating FcγR (FcγRI, III, and IV) has resulted in reduced atherosclerotic lesions in hyperlipidemic apoE KO mouse model. The attenuated lesions in apoE-Fcγ chain DKO mice are not due to the imbalance in Th1/Th2 shift. On the contrary, our findings showed higher Tregs with a concomitant decrease in Th17 cells, in part contributed to the abridged lesions in Fcγ chain deficient mice in hyperlipidemic conditions. Importantly, reduced FcγR-mediated IL-6 secretion may contribute to attenuated Th17 response and subsequently attenuated atherosclerosis in apoE-Fcγ chain-DKO mice. These studies collectively suggest that the lack of IL-6 secretion in Fcγ chain-deficient mice may be contributing to the reduced number of Th17 cells in apoE-Fcγ chain DKO mice.

Acknowledgments

We thank John Gregan for his help with manuscript preparation. We thank Jessica Warden for the technical assistance.

REFERENCES

1. Steinberg D. Low density lipoprotein oxidation and its pathobiological significance. J. Biol. Chem. 1997; 272:20963–20966. [PubMed: 9261091]
2. Yla-Herttuala S, Palinski W, Butler SW, Picard S, Steinberg D, Witztum JL. Rabbit and human atherosclerotic lesions contain IgG that recognizes epitopes of oxidized LDL. Arteriosclerosis and Thrombosis. 1994; 14:32–40. [PubMed: 7506053]
3. Palinski W, Tangirala RK, Miller E, Young SG, Witztum JL. Increased autoantibody titers against epitopes of oxidized LDL in LDL receptor-deficient mice with increased atherosclerosis. Atertio. Thromb. Vasc. Biol. 1995; 15:1569–1576.

4. Salonen JT, Yla-Herttuala S, Yamamoto R, Butler S, Korpela H, Salonen R, Nyyssonen K, Palinski W, Witztum JL. Autoantibody against oxidized LDL and progression of carotid atherosclerosis. Lancet. 1992; 39:883–887. [PubMed: 1348295]

5. Bergmark C, Wu R, de Faire U, Lefvert AK, Swedenborg J. Patients with early-onset peripheral vascular disease have increased levels of autoantibodies against oxidized LDL. Atertio. Thromb. Vasc. Biol. 1995; 15:441–445.

6. Tsimikas S, Brilakis ES, Lennon RJ, Miller ER, Witztum JL, McConnell JP, Kornman KS, Berger PB. Relationship of IgG and IgM autoantibodies to oxidized low density lipoprotein with coronary artery disease and cardiovascular events. J. Lipid Res. 2007; 48:425–433. [PubMed: 17093289]

7. Bharadwaj D, Stein MP, Volzer M, Mold C, Du Clos TW. The major receptor for C-reactive protein on leukocytes is fcgamma receptor II. J Exp Med. 1999; 190:585–590. [PubMed: 10449529]

8. Ridker PM, Rifai N, Rose L, Buring JE, Cook NR. Comparison of C-reactive protein and low-density lipoprotein cholesterol levels in the prediction of first cardiovascular events. N Engl J Med. 2002; 347:1557–1565. [PubMed: 12432042]

9. Hashimoto H, Kitagawa K, Hougaku H, Shimizu Y, Sakaguchi M, Nagai Y, Iyama S, Yamanishi H, Matsumoto M, Hori M. C-reactive protein is an independent predictor of the rate of increase in early carotid atherosclerosis. Circulation. 2001; 104:63–67. [PubMed: 11435339]

10. Teupser D, Weber O, Rao TN, Sass K, Thiery J, Fehling HJ. No reduction of atherosclerosis in C-reactive protein (CRP)-deficient mice. J Biol Chem. 2011; 286:6272–6279. [PubMed: 21149301]

11. Hulett MD, Hogarth PM. Molecular basis of Fc receptor function. Adv. Immunol. 1994; 57:1–127. [PubMed: 7872156]

12. Ravetch JV, Lanier LL. Immune inhibitory receptors. Science. 2000; 290:84–89. [PubMed: 11021804]

13. Ravetch JV, Bolland S. IgG Fc Receptors. Annu. Rev. Immunol. 2001; 19:275–290. [PubMed: 11244038]

14. Kurosaki T, Gander I, Ravetch JV. A subunit common to an IgG Fc receptor and the T-cell receptor mediates assembly through different interactions. Proceedings of the National Academy of Sciences of the United States of America. 1991; 88:3837–3841. [PubMed: 1827205]

15. Nagarajan S, Chesla SE, Cobern L, Anderson P, Zhu C, Selvaraj P. Ligand binding and phagocytosis by CD16 (Fc gamma receptor III) isoforms. J. Biol. Chem. 1995; 270:25762–25770. [PubMed: 7592758]

16. Takai T, Li M, Sylvestre D, Clynes R, Ravetch JV. FcR gamma chain deletion results in pleiotrophic effector cell defects. Cell. 1994; 76:519–529. [PubMed: 8313472]

17. Clynes R, Dumitru C, Ravetch JV. Uncoupling of immune complex formation and kidney damage in autoimmune glomerulonephritis. Science. 1998; 279:1052–1054. [PubMed: 9461440]

18. Jonasson L, Holm J, Skalli O, Bondjers G, Hansson GK. Regional accumulations of T cells, macrophages, and smooth muscle cells in the human atherosclerotic plaque. Arteriosclerosis. 1986; 6:131–138. [PubMed: 2937395]

19. Zhou X, Paulsson G, Stemme S, Hansson GK. Hypercholesterolemia is associated with a T helper (Th) 1/Th2 switch of the autoimmune response in atherosclerotic apo E-knockout mice. J. Clin. Invest. 1998; 101:1717–1725. [PubMed: 9541503]

20. Nagarajan S. Anti-OxLDL IgG blocks OxLDL interaction with CD36, but promotes FcgammaR, CD32A-dependent inflammatory cell adhesion. Immunol. Lett. 2007; 108:52–61. [PubMed: 17081622]

21. Raaz D, Herrmann M, Ekici AB, Klinghammer L, Lausen B, Voll RE, Leusen JH, van de Winkel JG, Daniel WG, Reis A, Garlichs CD. FcgammaRIIa genotype is associated with acute coronary syndromes as first manifestation of coronary artery disease. Atherosclerosis. 2009; 205:512–516. [PubMed: 19232413]

22. Hernandez-Vargas P, Ortiz-Munoz G, Lopez-Franco O, Suzuki Y, Gallego-Delgado J, Sanjuan G, Lazaro A, Lopez-Parra V, Ortega L, Egido J, Gomez-Guerrero C. Fcgamma receptor deficiency confers protection against atherosclerosis in apolipoprotein E knockout mice. Circul. Res. 2006; 99:1188–1196.

23. Kelly JA, Griffin ME, Fava RA, Wood SG, Bessette KA, Miller ER, Huber SA, Binder CJ, Witztum JL, Morganelli PM. Inhibition of arterial lesion progression in CD16-deficient mice:

evidence for altered immunity and the role of IL-10. Cardiovascular Research. 2010; 85:224–231. [PubMed: 19720605]

24. Zhao M, Wigren M, Duner P, Kolbus D, Olofsson KE, Bjorkbacka H, Nilsson J, Fredrikson GN. FcgammaRIIB inhibits the development of atherosclerosis in low-density lipoprotein receptor-deficient mice. J. Immunol. 2010; 184:2253–2260. [PubMed: 20097865]
25. Mendez-Fernandez YV, Stevenson BG, Diehl CJ, Braun NA, Wade NS, Covarrubias R, van Leuven S, Witztum JL, Major AS. The inhibitory FcgammaRIIb modulates the inflammatory response and influences atherosclerosis in male apoE(−/−) mice. Atherosclerosis. 2011; 214:73–80. [PubMed: 21084088]
26. Zhou X, Nicoletti A, Elhage R, Hansson GK. Transfer of CD4(+) T cells aggravates atherosclerosis in immunodeficient apolipoprotein E knockout mice. Circulation. 2000; 102:2919–2922. [PubMed: 11113040]
27. Zhou X, Robertson AK, Hjerpe C, Hansson GK. Adoptive transfer of CD4+ T cells reactive to modified low-density lipoprotein aggravates atherosclerosis. Atertio. Thromb. Vasc. Biol. 2006; 26:864–870.
28. Thampi P, Stewart BW, Joseph L, Melnyk SB, Hennings LJ, Nagarajan S. Dietary homocysteine promotes atherosclerosis in apoE-deficient mice by inducing scavenger receptors expression. Atherosclerosis. 2008; 197:620–629. [PubMed: 17950295]
29. Lutz MB, Kukutsch N, Ogilvie AL, Rossner S, Koch F, Romani N, Schuler G. An advanced culture method for generating large quantities of highly pure dendritic cells from mouse bone marrow. J Immunol Methods. 1999; 223:77–92. [PubMed: 10037236]
30. Marim FM, Silveira TN, Lima DS Jr, Zamboni DS. A method for generation of bone marrow-derived macrophages from cryopreserved mouse bone marrow cells. PLoS One. 2010; 5:e15263. [PubMed: 21179419]
31. Devaraj S, Du Clos TW, Jialal I. Binding and internalization of C-reactive protein by Fcgamma receptors on human aortic endothelial cells mediates biological effects. Atertio. Thromb. Vasc. Biol. 2005; 25:1359–1363.
32. Wu J, Stevenson MJ, Brown JM, Grunz EA, Strawn TL, Fay WP. C-reactive protein enhances tissue factor expression by vascular smooth muscle cells: mechanisms and in vivo significance. Atertio. Thromb. Vasc. Biol. 2008; 28:698–704.
33. Szabo SJ, Kim ST, Costa GL, Zhang X, Fathman CG, Glimcher LH. A novel transcription factor, T-bet, directs Th1 lineage commitment. Cell. 2000; 100:655–669. [PubMed: 10761931]
34. Zheng W, Flavell RA. The transcription factor GATA-3 is necessary and sufficient for Th2 cytokine gene expression in CD4 T cells. Cell. 1997; 89:587–596. [PubMed: 9160750]
35. Erbel C, Chen L, Bea F, Wangler S, Celik S, Lasitschka F, Wang Y, Bockler D, Katus HA, Dengler TJ. Inhibition of IL-17A attenuates atherosclerotic lesion development in apoE-deficient mice. J. Immunol. 2009; 183:8167–8175. [PubMed: 20007582]
36. Smith E, Prasad KM, Butcher M, Dobrian A, Kolls JK, Ley K, Galkina E. Blockade of interleukin-17A results in reduced atherosclerosis in apolipoprotein E-deficient mice. Circulation. 2010; 121:1746–1755. [PubMed: 20368519]
37. Xie JJ, Wang J, Tang TT, Chen J, Gao XL, Yuan J, Zhou ZH, Liao MY, Yao R, Yu X, Wang D, Cheng Y, Liao YH, Cheng X. The Th17/Treg functional imbalance during atherogenesis in ApoE(−/−) mice. Cytokine. 2010; 49:185–193. [PubMed: 19836260]
38. Bettelli E, Carrier Y, Gao W, Korn T, Strom TB, Oukka M, Weiner HL, Kuchroo VK. Reciprocal developmental pathways for the generation of pathogenic effector TH17 and regulatory T cells. Nature. 2006; 441:235–238. [PubMed: 16648838]
39. Veldhoen M, Hocking RJ, Atkins CJ, Locksley RM, Stockinger B. TGFbeta in the context of an inflammatory cytokine milieu supports de novo differentiation of IL-17-producing T cells. Immunity. 2006; 24:179–189. [PubMed: 16473830]
40. Mangan PR, Harrington LE, O'Quinn DB, Helms WS, Bullard DC, Elson CO, Hatton RD, Wahl SM, Schoeb TR, Weaver CT. Transforming growth factor-beta induces development of the T(H)17 lineage. Nature. 2006; 441:231–234. [PubMed: 16648837]
41. Bettelli E, Oukka M, Kuchroo VK. T(H)-17 cells in the circle of immunity and autoimmunity. Nat Immunol. 2007; 8:345–350. [PubMed: 17375096]

42. Ogura H, Murakami M, Okuyama Y, Tsuruoka M, Kitabayashi C, Kanamoto M, Nishihara M, Iwakura Y, Hirano T. Interleukin-17 promotes autoimmunity by triggering a positive-feedback loop via interleukin-6 induction. Immunity. 2008; 29:628–636. [PubMed: 18848474]
43. Wei L, Laurence A, Elias KM, O'Shea JJ. IL-21 is produced by Th17 cells and drives IL-17 production in a STAT3-dependent manner. J Biol Chem. 2007; 282:34605–34610. [PubMed: 17884812]
44. Zhou L, Ivanov II, Spolski R, Min R, Shenderov K, Egawa T, Levy DE, Leonard WJ, Littman DR. IL-6 programs T(H)-17 cell differentiation by promoting sequential engagement of the IL-21 and IL-23 pathways. Nat Immunol. 2007; 8:967–974. [PubMed: 17581537]
45. Torchinsky MB, Garaude J, Martin AP, Blander JM. Innate immune recognition of infected apoptotic cells directs T(H)17 cell differentiation. Nature. 2009; 458:78–82. [PubMed: 19262671]
46. Palinski W, Miller E, Witztum JL. Immunization of low density lipoprotein (LDL) receptor-deficient rabbits with homologous malondialdehyde-modified LDL reduces atherogenesis. Proceedings of the National Academy of Sciences of the United States of America. 1995; 92:821–825. [PubMed: 7846059]
47. Ameli S, Hultgardh-Nilsson A, Regnstrom J, Calara F, Yano J, Cercek B, Shah PK, Nilsson J. Effect of immunization with homologous LDL and oxidized LDL on early atherosclerosis in hypercholesterolemic rabbits. Atertio. Thromb. Vasc. Biol. 1996; 16:1074–1079.
48. Zhou X, Caligiuri G, Hamsten A, Lefvert AK, Hansson GK. LDL immunization induces T-cell-dependent antibody formation and protection against atherosclerosis. Atertio. Thromb. Vasc. Biol. 2001; 21:108–114.
49. van Es T, van Puijvelde GH, Ramos OH, Segers FM, Joosten LA, van den Berg WB, Michon IM, de Vos P, van Berkel TJ, Kuiper J. Attenuated atherosclerosis upon IL-17R signaling disruption in LDLr deficient mice. Biochem Biophys Res Commun. 2009; 388:261–265. [PubMed: 19660432]
50. Chen S, Shimada K, Zhang W, Huang G, Crother TR, Arditi M. IL-17A is proatherogenic in high-fat diet-induced and Chlamydia pneumoniae infection-accelerated atherosclerosis in mice. J Immunol. 2010; 185:5619–5627. [PubMed: 20935201]
51. Taleb S, Romain M, Ramkhelawon B, Uyttenhove C, Pasterkamp G, Herbin O, Esposito B, Perez N, Yasukawa H, Van Snick J, Yoshimura A, Tedgui A, Mallat Z. Loss of SOCS3 expression in T cells reveals a regulatory role for interleukin-17 in atherosclerosis. J Exp Med. 2009; 206:2067–2077. [PubMed: 19737863]
52. Ait-Oufella H, Herbin O, Bouaziz JD, Binder CJ, Uyttenhove C, Laurans L, Taleb S, Van Vre E, Esposito B, Vilar J, Sirvent J, Van Snick J, Tedgui A, Tedder TF, Mallat Z. B cell depletion reduces the development of atherosclerosis in mice. J Exp Med. 2010; 207:1579–1587. [PubMed: 20603314]
53. Yang X, Nurieva OR, Martinez GJ, Kang HS, Chung Y, Pappu BP, Shah B, Chang SH, Schluns KS, Watowich SS, Feng XH, Jetten AM, Dong C. Molecular antagonism and plasticity of regulatory and inflammatory T cell programs. Immunity. 2008; 29:44–56. [PubMed: 18585065]
54. Xu L, Kitani A, Fuss I, Strober W. Cutting edge: regulatory T cells induce CD4+CD25-Foxp3- T cells or are self-induced to become Th17 cells in the absence of exogenous TGF-beta. J Immunol. 2007; 178:6725–6729. [PubMed: 17513718]
55. de Boer OJ, van der Meer JJ, Teeling P, van der Loos CM, van der Wal AC. Low numbers of FOXP3 positive regulatory T cells are present in all developmental stages of human atherosclerotic lesions. PLoS One. 2007; 2:e779. [PubMed: 17712427]
56. Cheng X, Yu X, Ding YJ, Fu QQ, Xie JJ, Tang TT, Yao R, Chen Y, Liao YH. The Th17/Treg imbalance in patients with acute coronary syndrome. Clin. Immunol. 2008; 127:89–97. [PubMed: 18294918]
57. de Boer OJ, van der Meer JJ, Teeling P, van der Loos CM, Idu MM, van Maldegem F, Aten J, van der Wal AC. Differential expression of interleukin-17 family cytokines in intact and complicated human atherosclerotic plaques. J. Pathol. 2010; 220:499–508. [PubMed: 20020510]
58. Pinderski Oslund LJ, Hedrick CC, Olvera T, Hagenbaugh A, Territo M, Berliner JA, Fyfe AI. Interleukin-10 blocks atherosclerotic events in vitro and in vivo. Atertio. Thromb. Vasc. Biol. 1999; 19:2847–2853.

59. Robertson AK, Rudling M, Zhou X, Gorelik L, Flavell RA, Hansson GK. Disruption of TGF-beta signaling in T cells accelerates atherosclerosis. J. Clin. Invest. 2003; 112:1342–1350. [PubMed: 14568988]

60. Frutkin AD, Otsuka G, Stempien-Otero A, Sesti C, Du L, Jaffe M, Dichek HL, Pennington CJ, Edwards DR, Nieves-Cintron M, Minter D, Preusch M, Hu JH, Marie JC, Dichek DA. TGF-[beta]1 limits plaque growth, stabilizes plaque structure, and prevents aortic dilation in apolipoprotein E-null mice. Atertio. Thromb. Vasc. Biol. 2009; 29:1251–1257.

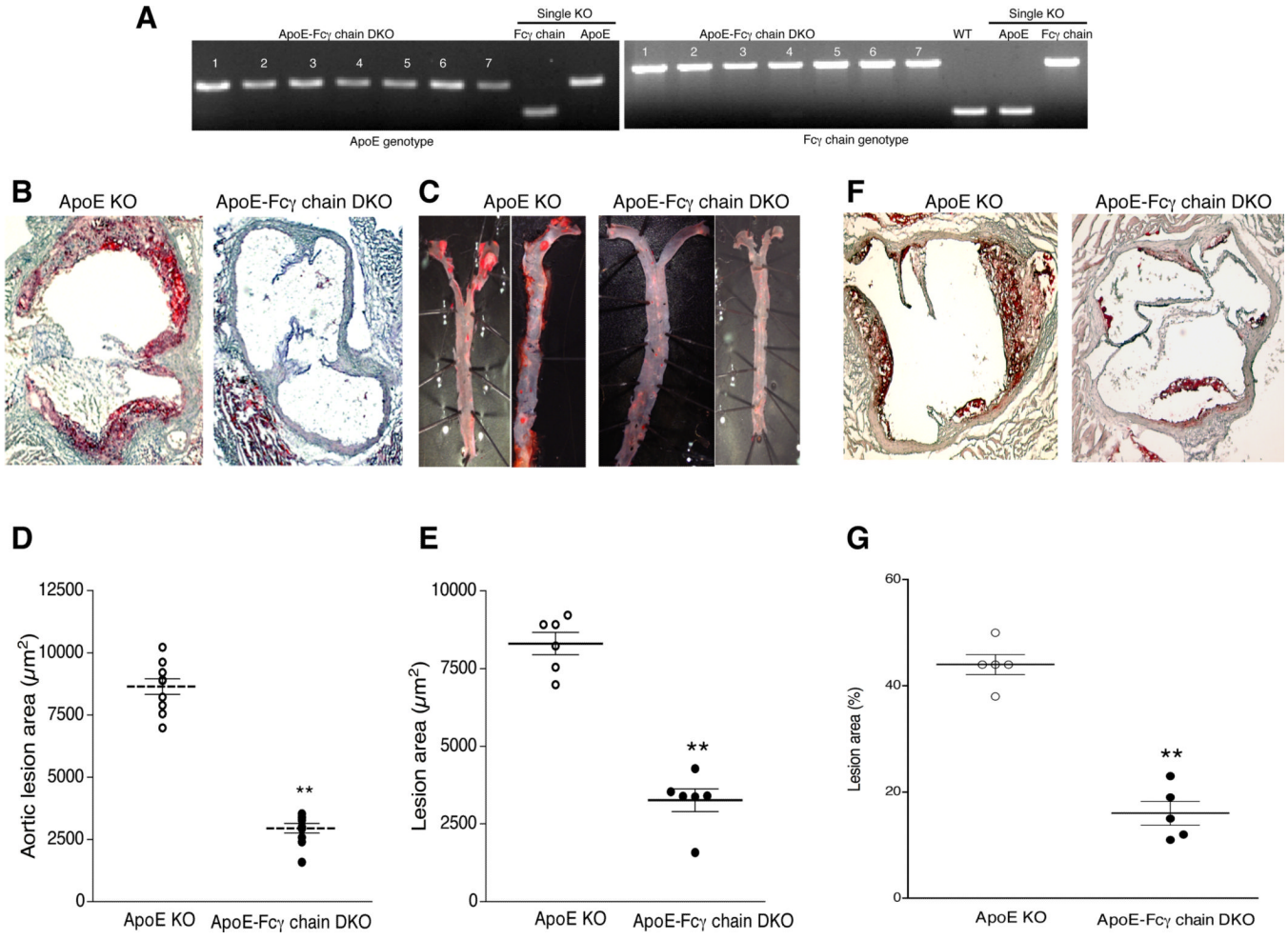

Figure 1. ApoE-Fcγ chain DKO mice show reduced atherosclerotic lesions

A, Genotype analyses for *apoE* (left) and *Fcγ* chain (right) was determined by PCR using DNA isolated from apoE-Fcγ chain DKO mice colony. Wild type (WT), Fcγ chain KO, and apoE KO (single knockout) were used as controls. Number indicates number of mice used for the analyses. ***B***, Representative aortic sinus sections from apoE KO and apoE-Fcγ chain DKO mice fed chow diet were stained with Oil Red O to determine fatty streak lesions. ***C***, Atherosclerotic lesions in the descending aorta of apoE KO and apoE-Fcγ chain DKO mice fed chow diet was determined after staining descending aorta with Sudan IV. Representative of two aorta from apoE KO and apoE-Fcγ chain DKO were presented. Quantitative analysis of atherosclerotic lesions in aortic sinus (***D***) and descending aorta (***E***) were determined as described under 'methods'. Each group contained 8 mice. *F*, Fcγ chain deficiency reduces high-fat induced atherosclerotic lesions. Aortic sinus sections from apoE KO and apoE-Fcγ chain DKO mice fed high fat diet for 10 wk were stained with oil Red O. *G*, Quantification of aortic sinus lesions from apoE KO and apoE-Fcγ chain DKO mice fed high fat diet were determined as described under 'methods'. Each group for the high fat fed study contained 5 mice. ***p* <0.01 compared to apoE KO mice.

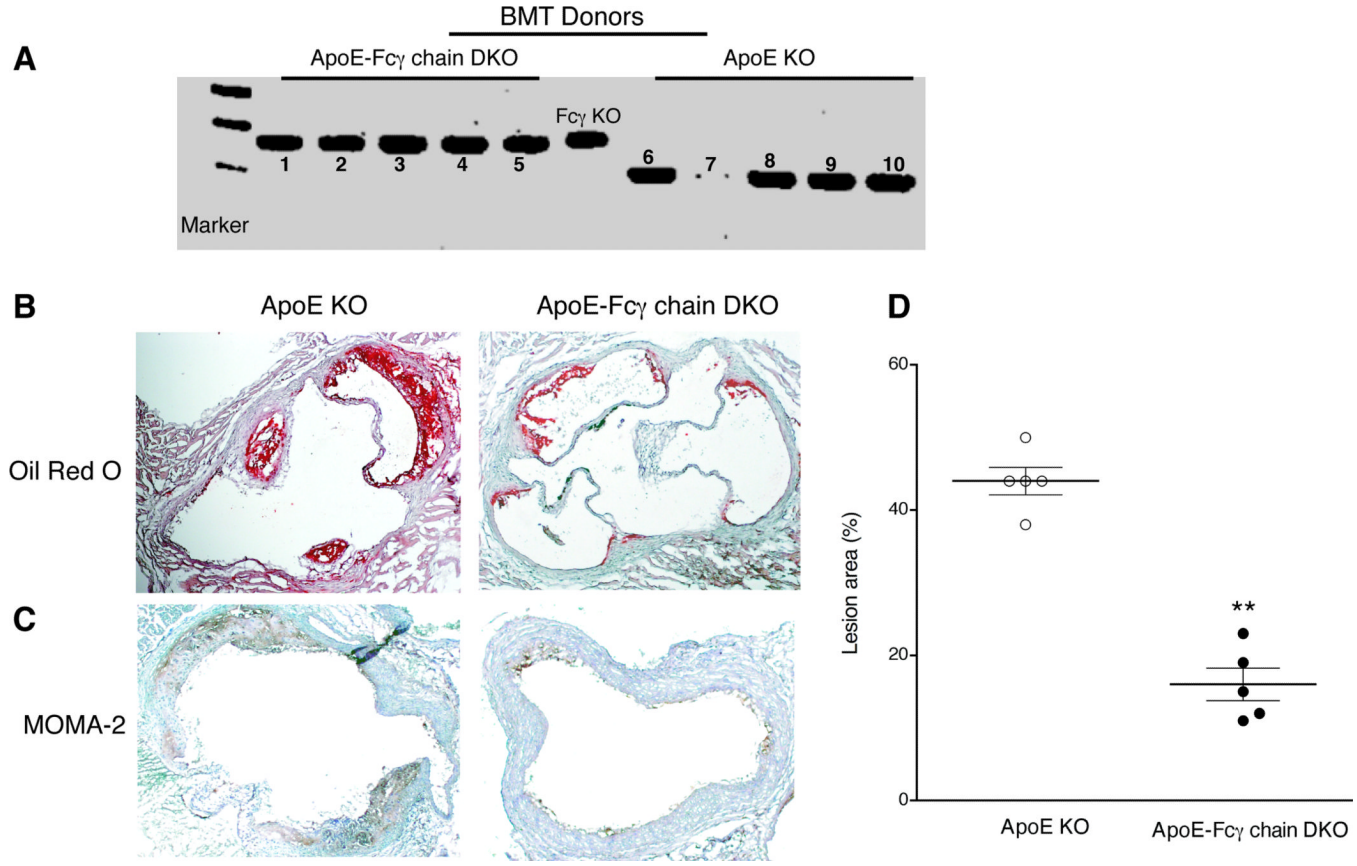

Figure 2. Activating FcγR expressed on hematopoietic cells is sufficient to contribute to the atherosclerotic lesions

A, Bone marrow chimera analysis of peripheral leukocytes for Fcγ chain deficiency were determined by genomic PCR. DNA from apoE KO mice (n=10) received apoE-Fcγ chain DKO (left panel, 1–5) or apoE KO (right panel, 6–10) bone marrow were used to amplify Fcγ chain by PCR using wild type and mutant Fcγ chain primers as described under 'methods'. DNA from apoE-Fcγ chain mice tail DNA was used as a positive control. Genotype analyses for *apoE* (left) and *Fcγ* chain (right) was determined by PCR using DNA isolated from apoE-Fcγ chain DKO mice colony. Wild type (WT), Fcγ chain KO, and apoE KO (single knockout) were used as controls. ***B***, Aortic sinus sections from apoE KO mice received apoE KO or apoE-Fcγ chain DKO mice bone marrow. After bone marrow transplantation recipient mice were fed high fat diet for 10 wk. ***C***, Representative aortic sinus sections from apoE KO mice received apoE KO or apoE-Fcγ chain DKO mice bone marrow were stained with anti-mouse macrophage mAb (MOMA-2) for the detection of macrophages at the lesion site. Representative of five aortic sinus sections from apoE KO and apoE-Fcγ chain DKO were presented. Aortic sinus sections stained with isotype control rat IgG2b did not show any positive staining (data not shown). Quantitative analysis of atherosclerotic lesions in aortic sinus (***D***) of bone marrow chimera mice was determined as described under 'methods'. Each group contained 5 mice. ***p* <0.01 compared to apoE KO mice.

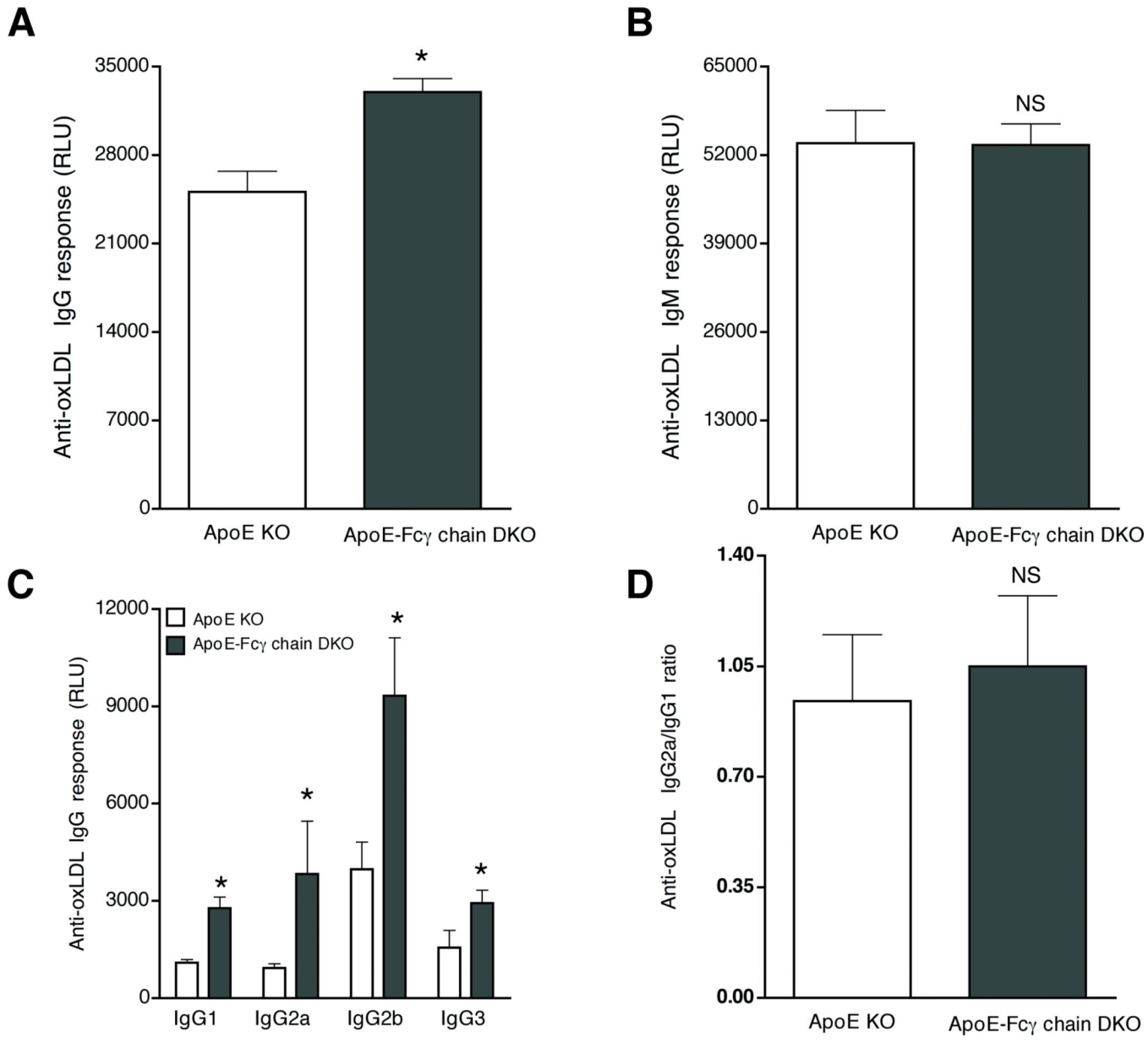

Figure 3. Elevated anti-oxLDL IgG levels in apoE-Fcγ chain DKO mice

Anti-oxLDL IgG (***A***) and IgM (***B***) levels were determined in sera from apoE KO and apoE-Fcγ chain DKO mice fed high fat diet for 10 wks. Sera were diluted 1:200 and 1:500 to determine anti-oxLDL IgG and anti-oxLDL IgM levels. Each value indicates mean ± SD results from five mice. ***C***, Anti-oxLDL IgG isotype analysis was determined in sera from apoE KO and apoE-Fcγ chain DKO mice fed high fat diet for 10 wks. Sera was diluted 1:50 and anti-oxLDL IgG1, IgG2a, IgG2b and IgG3 levels were determined using isotype specific secondary antibodies. In all these assays lumophos530, a luminescence alkaline phosphatase substrate, was used and relative light units (RLU) was measured in a luminescence plate reader. Each group contained 5 mice. ***D***, IgG1/IgG2a ratio was determined arbitrarily by taking a ratio between the RLU values obtained for each animal. Each group contained 5 mice. NS, not significant and **p* <0.05 and compared to apoE KO mice.

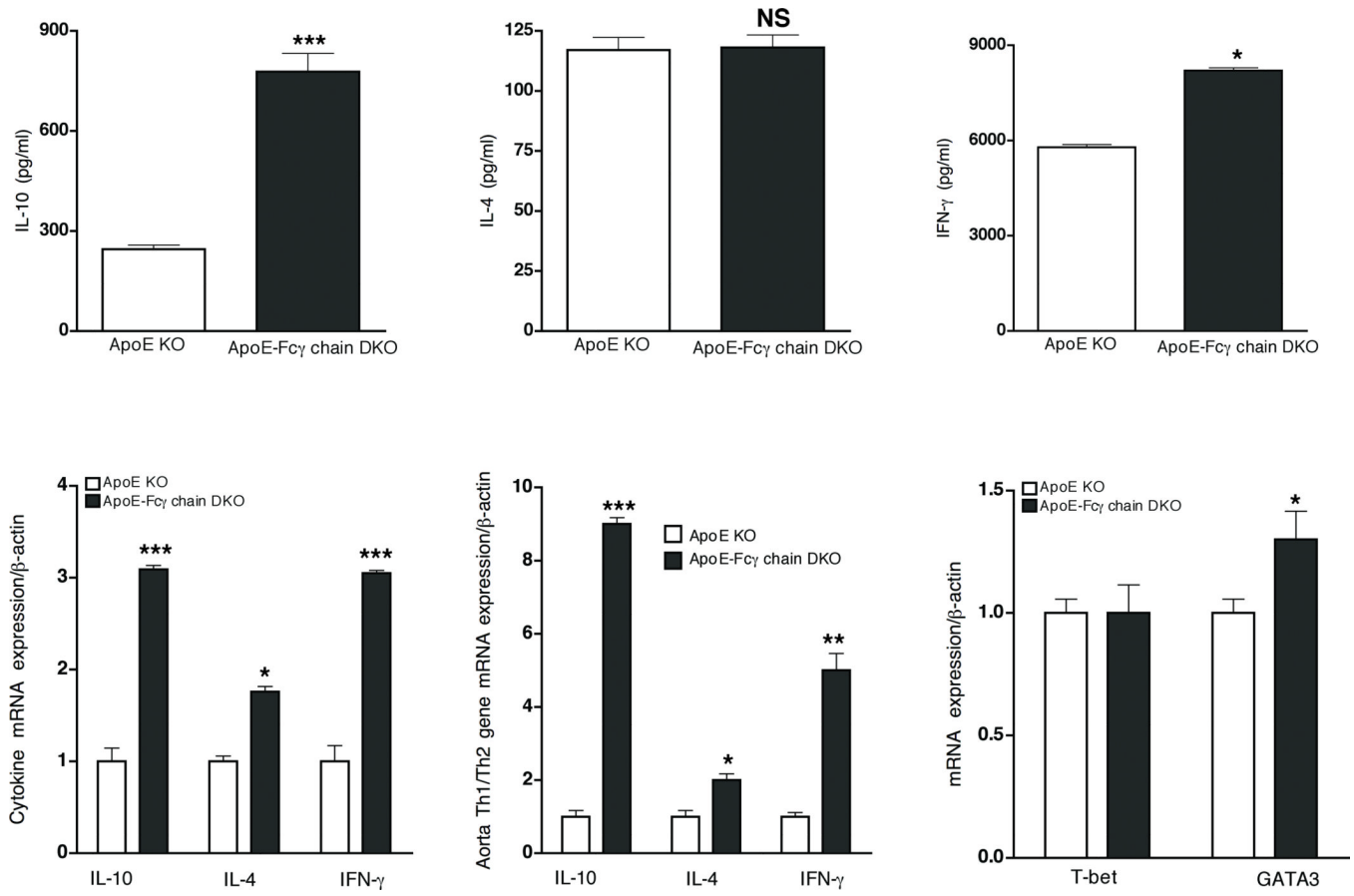

Figure 4. Attenuated atherosclerotic lesion in apoE-Fcγ chain DKO mice is not due to Th1/Th2 shift

CD4 T cell responses in apoE-Fcγ chain DKO and apoE KO mice fed high fat diet. Purified CD4+ lymphocytes were stimulated with plate-bound anti-CD3 and soluble CD28 for 72 h. The concentration of IL-10 (***A***), IL-4 (***B***), and IFN-γ (***C***) were measured by cytokine bead array. Each value indicates mean ± SD results from 5 mice. ***D***, Th1/Th2 cytokine transcript expression by CD4+ cells. RNA was isolated from purified CD4+ cells of apoE KO and apoE-Fcγ chain DKO mice fed high fat diet for 10 wks. IL-10, IL-4 and IFN-γ mRNA levels were determined by quantitative RT-PCR assays and normalized relative to housekeeping gene, β-actin transcripts. Each value indicates mean ± SD results from five mice. ***E***, Th1/Th2 cytokine mRNA expression in aorta. RNA was isolated from descending aorta and IL-10, IL-4 and IFN-γ mRNA expression were determined by quantitative RT-PCR analysis. Cytokine mRNA expression was normalized relative to β-actin mRNA expression. Values are expressed as means ± SD, n=5/group. ***F,*** T-bet and GATA3 mRNA expression in CD4+ T cells. Basal expression of T-bet and GATA-3 mRNA levels were determined by quantitative RT-PCR assays and normalized relative to housekeeping gene, β-actin transcripts. Each value indicates mean ± SD results from five mice. NS, not significant, *p <0.05, **p <0.01, ***p <0.0001 compared to apoE KO mice.

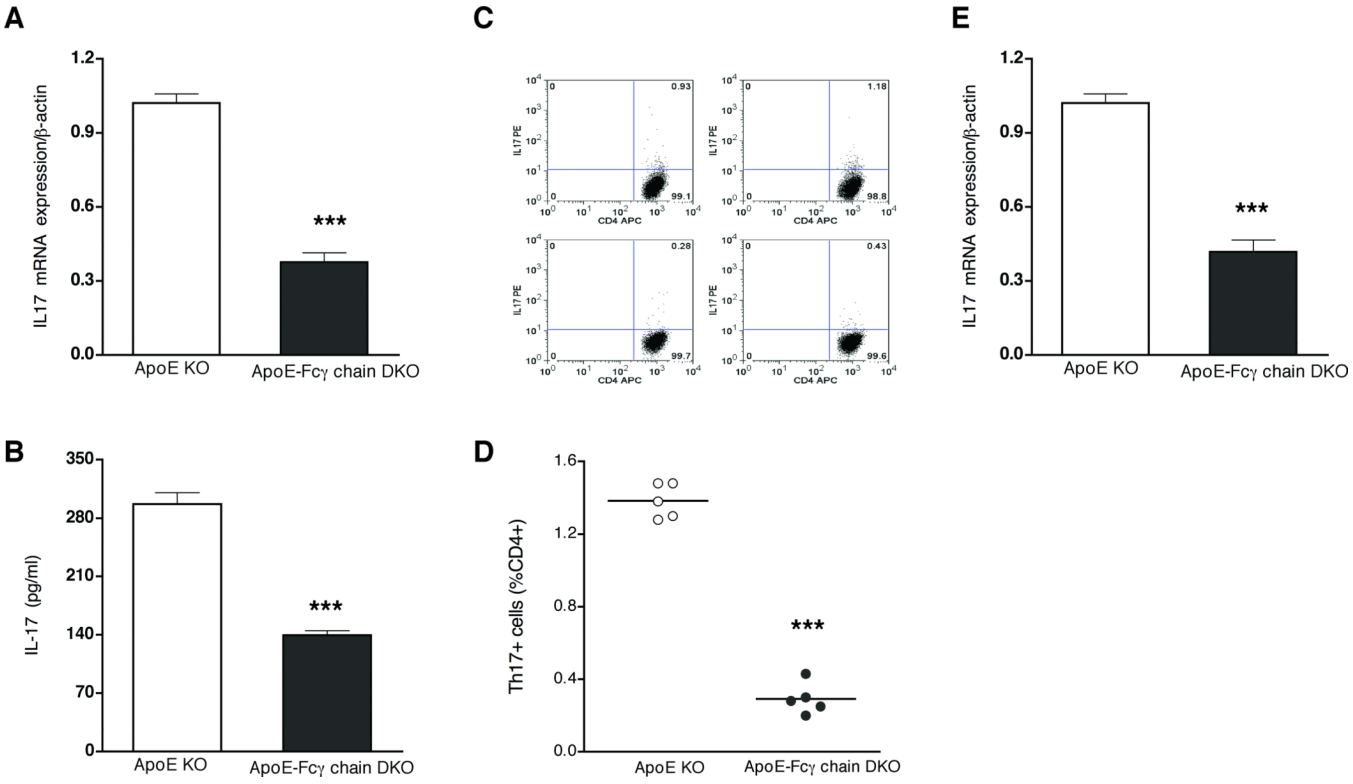

Figure 5. Th17 CD4+ T cells were reduced in apoE-Fcγ DKO mice

RNA was isolated from purified CD4+ cells of apoE KO and apoE-Fcγ chain DKO mice fed high fat diet for 10 wks. IL-17A mRNA levels (***A***) were determined by quantitative RT-PCR assays and normalized relative to housekeeping gene, β-actin transcripts. Each value indicates mean ± SD results from five mice. ***B***, IL-17 secretion is reduced in apoE-Fcγ chain DKO mice fed high fat diet. Purified CD4+ lymphocytes from apoE KO and apoE-Fcγ chain DKO mice were stimulated with plate-bound anti-CD3 and soluble CD28 for 72 h. The concentration of IL-17 was measured by cytokine bead array. Each value indicates mean ± SD results from 5 mice. ***C and D***, Th17 cell number was reduced in apoE-Fcγ chain DKO mice. CD4+ cells were stimulated with PMA/ionomycin and CD4+IL17+ cells were determined by intracellular staining for IL-17 as described under “methods.” Representative flow cytometric analysis of Th17 cells (***C***) was presented. Quantification of number of CD4+IL17+ cells was determined by analyzing the FACS data using FlowJo software. Each value indicates mean ± SD results from five mice. *** p <0.001 compared to apoE KO mice. ***E***, IL-17A mRNA expression in aorta was determined by quantitative RT-PCR analysis. Values are expressed as means ± SD, n=5/group.

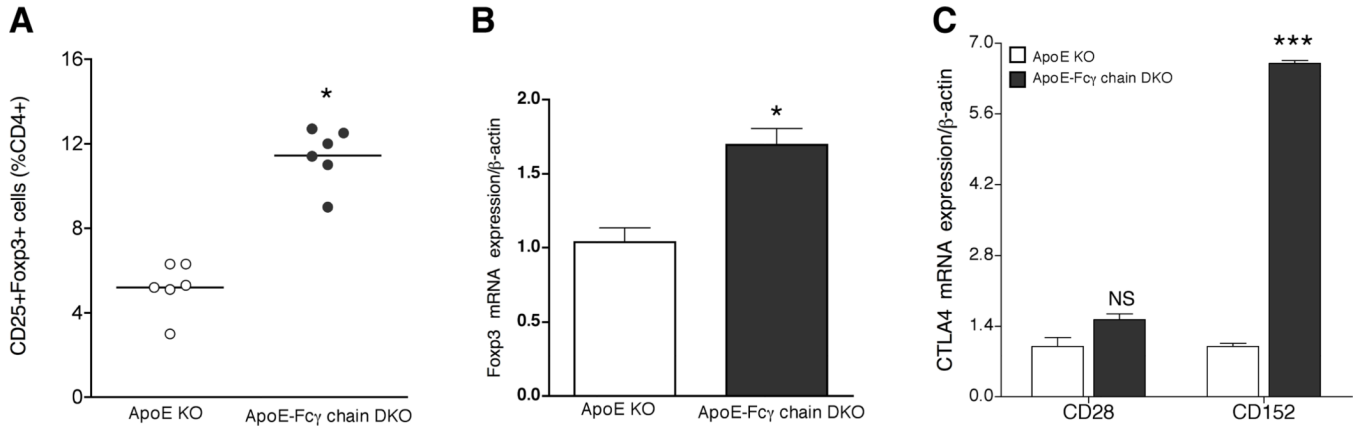

Figure 6. Number of Tregs was high in apoE-Fcγ chain DKO deficient mice

A, Flow cytometric analysis of CD4+CD25+Foxp3+ cells was determined by staining purified CD4 cells from apoE KO and apoE-Fcγ chain DKO mice fed high fat diet for 10 wks. Number of Tregs was determined by analyzing the FACS data using FlowJo software. ***B***, Foxp3 mRNA expression was high in CD4+ cells from apoE-Fcγ chain DKO mice. RNA was isolated from purified CD4+ cells of apoE KO and apoE-Fcγ chain DKO mice fed high fat diet for 10 wks. Foxp3 mRNA levels were determined by quantitative RT-PCR assays and normalized relative to housekeeping gene, β-actin transcripts. Each value indicates mean ± SD results from five mice. ***C***, CD152 mRNA expression was high in CD4+ cells from apoE-Fcγ chain DKO mice. RNA was isolated from purified CD4+ cells of apoE KO and apoE-Fcγ chain DKO mice fed high fat diet for 10 wks. CTLA4 and CD28 mRNA levels were determined by quantitative RT-PCR assays and normalized relative to housekeeping gene, β-actin transcripts. Each value indicates mean ± SD results from five mice. NS, not significant, *p <0.05, and, ***p <0.0001 compared to apoE KO mice.

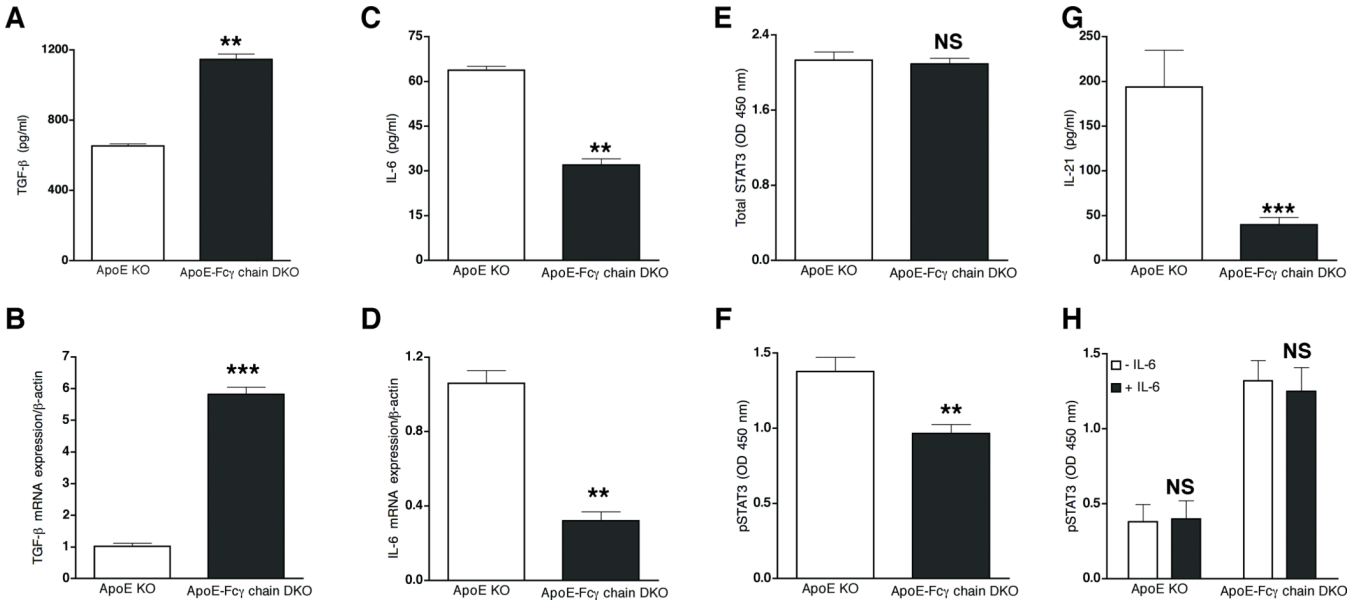

Figure 7. Reduced Th17 and higher Tregs is due to attenuated IL-6 expression

Purified CD4+ lymphocytes from apoE KO and apoE-Fcγ chain DKO (fed high fat diet for 10 wk) were stimulated with plate-bound anti-CD3 and soluble CD28 for 72 h. The concentration of TGF-β (***A***) and IL-6 (***B***) was measured by cytokine bead array. Each value indicates mean ± SD results from 5 mice. TGF-β (***C***) and IL-6 (***D***) mRNA expression in CD4+ cells from apoE-Fcγ chain DKO mice. RNA was isolated from purified CD4+ cells of apoE KO and apoE-Fcγ chain DKO mice fed high fat diet for 10 wks. TGF-β and IL-6 mRNA levels were determined by quantitative RT-PCR assays and normalized relative to housekeeping gene, β-actin transcripts. Each value indicates mean ± SD results from five mice. ***E, and F***, Reduced STAT-3 phosphorylation in ApoE-Fcγ chain DKO mice. Purified CD4 cells were stimulated with plate bound CD3 and cell lysates were prepared. Total STAT (***E***) and phospho-STAT3 (***F***) were determined by Pathscan ELISA kit as described under methods. ***G***, IL-21 secretion by activated CD4+ cells from apoE KO and apoE-Fcγ chain DKO mice fed high fat diet for 10 wks was determined by ELISA. Each value indicates mean ± SD results from 5 mice. ***H***, IL-6 induced STAT-3 phosphorylation in ApoE-Fcγ chain DKO mice. Purified CD4 cells of apoE KO and apoE-Fcγ chain DKO mice were stimulated without or with IL-6 and phospho-STAT3 were determined by Pathscan ELISA kit as described under methods. Values are expressed as means ± SD, n=5/group. NS, not significant, ** p <0.01, *** p <0.0001 compared to apoE KO mice.

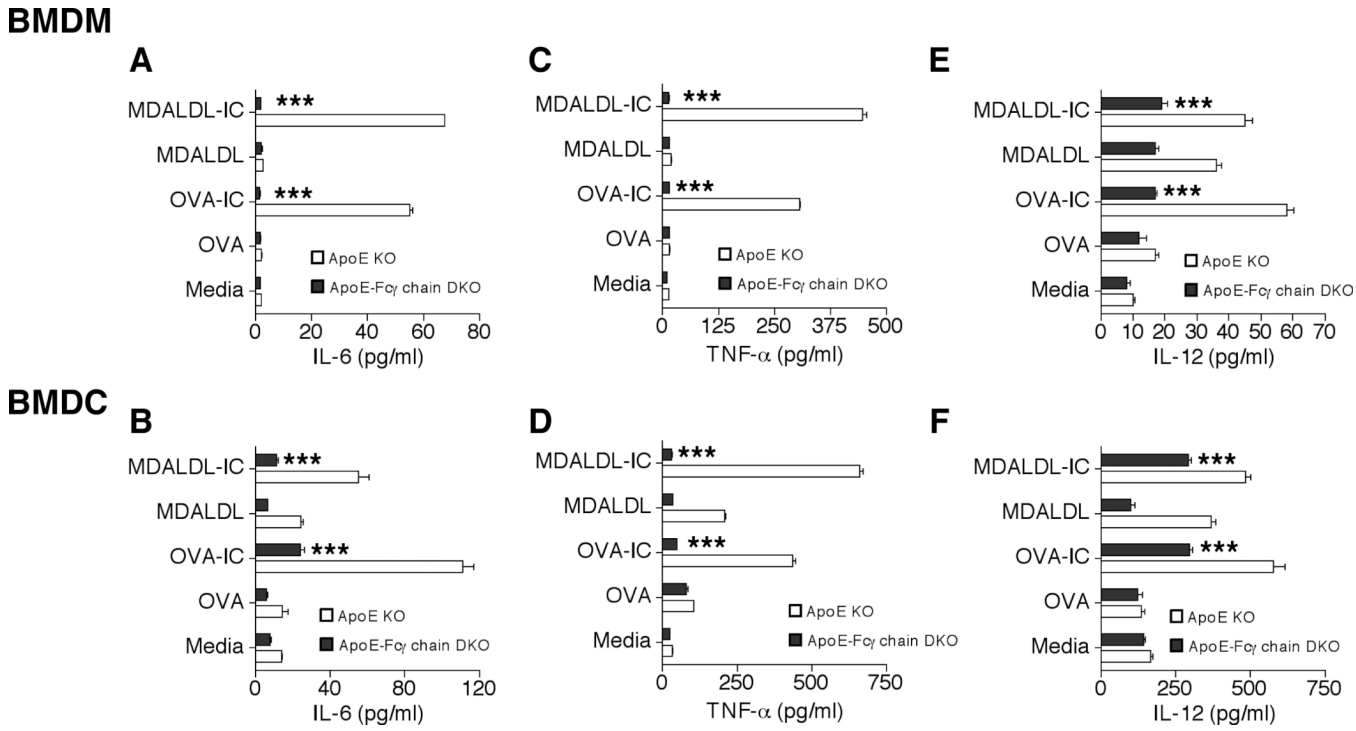

Figure 8. Reduced IL6 secretion by BMDM and BMDC of apoE-Fcγ chain DKO mice

BMDM and BMDC from apoE KO and apoE-Fcγ chain DKO mice were stimulated with plate-bound OVA-IC or MDALDL-IC for 24 h. Secretion of IL-6 (A, B), TNF-α (C, D) and IL-12 (E, F) by BMDM and BMDC was measured by corresponding Duoset ELISA kits. Each value indicates mean ± SD results from triplicates. ****p* <0.0001 compared to apoE KO mice.

TABLE I

Plasma lipid concentrations in apoE KO and apoE-Fcγ chain DKO mice

	Chow diet[1]		High fat[1]		BMT High fat[2]	
	Cholesterol (mg/dL)	**HDL (mg/dL)**	**Cholesterol (mg/dL)**	**HDL (mg/dL)**	**Cholesterol (mg/dL)**	**HDL (mg/dL)**
ApoE KO	565 ± 46	26 ± 2	1051 ± 137	23.0 ± 3.0	994 ± 65	26.8 ± 6.3
ApoE-Fcγ chain DKO	603 ± 66	33 ± 5	1061 ± 159	22.6 ± 3.4	1020 ± 75	32.6 ± 2.8

[1] Values are means ± SD, n=10 and

[2] n=5.